Limnology (2000) 1:107–115

RESEARCH PAPER

Ross F. Walker · Michio Kumagai

Image analysis as a tool for quantitative phycology: a computational approach to cyanobacterial taxa identification

Received: September 6, 1999 / Accepted: February 6, 2000

Abstract In the following work we discuss the application of image processing and pattern recognition to the field of quantitative phycology. We overview the area of image processing and review previously published literature pertaining to the image analysis of phycological images and, in particular, cyanobacterial image processing. We then discuss the main operations used to process images and quantify data contained within them. To demonstrate the utility of image processing to cyanobacteria classification, we present details of an image analysis system for automatically detecting and classifying several cyanobacterial taxa of Lake Biwa, Japan. Specifically, we initially target the genus *Microcystis* for detection and classification from among several species of *Anabaena*. We subsequently extend the system to classify a total of six cyanobacteria species. High-resolution microscope images containing a mix of the above species and other nontargeted objects are analyzed, and any detected objects are removed from the image for further analysis. Following image enhancement, we measure object properties and compare them to a previously compiled database of species characteristics. Classification of an object as belonging to a particular class membership (e.g., "*Microcystis*," "*A. smithii*," "*Other*," etc.) is performed using parametric statistical methods. Leave-one-out classification results suggest a system error rate of approximately 3%.

Key words Image processing · Pattern recognition · Phycology · Cyanobacteria · Classification

Introduction

The application of engineering techniques to phycology continues to play a growing role in understanding the complex physical and biological relationships between algae and their environments. A brief survey of the literature shows a steady rise in such applications since the early 1980s, influenced in part by the availability of powerful yet inexpensive computing systems. A further reason is the continuing worldwide deterioration of environmental health and a growing awareness among researchers and scholars that many areas of phycology (especially algae and its potential for environmental contamination) are little understood. The past 20 years have seen a slow but gradual increase in the frequency of use of image-processing techniques in the area of phycology and water analysis. Katsinis et al. (1984) used image processing to classify marine zooplankton into one of eight taxonomic groups, with 92% accuracy. In the same year, Jeffries et al. (1984) used image analysis to automatically count, size, and identify zooplankton, with a reported 90% accuracy. Estep et al. (1986) used image processing to determine the abundance, size, shape, volume, and surface area of microorganisms ranging from bacteria to fish larvae. Schultze-Lam et al. (1992) used electron microscopy and image analysis to quantify the role of the cyanobacteria *Synechococcus* spp. in lake mineral growth. More recently, artificial neural networks were used by Blackburn et al. (1998) and Wilkins et al. (1999) to classify images of stained bacterial plankton.

The increasing occurrence of algal bloom contamination in both lakes and sea serves as a worrying indicator of increasing environmental stress on water ecosystems. Lake Biwa, Japan's largest lake and source of drinking water for over thirteen million people, has experienced such blooms with increasing frequency over the last decade. The majority of these blooms are caused by three genera of cyanobacteria – *Microcystis*, *Anabaena*, and *Planktothrix* – as well as one species of Chrysophyceae, *Uroglena americana*. A telling contrast to the deteriorating condition of the lake's waters can be seen in Nakanishi's (1984) comprehensive review of Lake Biwa's 90 species of algae (including 12 Cyanophyceae), which makes no mention of cyanobacterial blooms.

In the summer of 1994, the influences of a severe drought and eutrophication produced serious algal blooms at vari-

R.F. Walker (✉) · M. Kumagai
Lake Biwa Research Institute, 1-10 Uchidehama, Otsu 520-0806, Japan
Tel. +81-77-526-4690; Fax +81-77-526-4803
e-mail: walker@lbri.go.jp

ous locations in Lake Biwa and other water bodies throughout Japan. Lake Biwa's Akanoi Bay was especially affected, with higher concentrations of cyanobacteria and longer bloom durations than elsewhere in the lake. There is strong potential for the cyanobacteria produced in Akanoi Bay to spread to a huge area of Lake Biwa (Kumagai 1996). To understand the environmental precursors to algal blooms and to allow corrective measures to be implemented prior to bloom manifestation, quantitative measurement of cyanobacteria species and population densities is essential. Such monitoring of water bodies (for the presence or absence of targeted species) usually involves the manual analysis of water samples by trained experts – a very time-consuming and, therefore, expensive operation. Because of this, considerable advantage can be gained by implementing an automated measurement system via image processing and pattern recognition. Recent advances in computer performance and image analysis now allow the possibility of assisted or "adjunct" screening of water samples by image processing and pattern recognition systems. However, this area of research has seen slow progress over the last decade, with very little published literature. Apart from Thiel (1994), there appear to be no other *major* published works or texts on this subject, and few active researchers are working on this significant problem. We feel that the rapid technological advances in high-speed computers and high-resolution digital cameras will yield systems usable in real-world applications.

In this paper, we detail the implementation and evaluation of an image processing system for automatically detecting and classifying cyanobacteria taxa and report classification results. We first introduce the topic of cyanobacteria image analysis and discuss several problems that make such analysis inherently difficult. We then discuss the hardware, software, and image processing technology that has resulted from the approximately 15-month life of this project. Finally, we present the significant results of our research and discuss relevant points that need further investigation.

Cyanobacteria image analysis

Although very similar to other forms of image analysis, cyanobacteria classification presents the image analyst with its own inherent difficulties. The dynamic and variable nature of the lake microcosm creates a formidable challenge to designing a robust pattern recognition system with the ideal characteristics of high analysis accuracy but with wide generalization ability. Below we discuss a number of these challenges:

Intraspecies variation due to natural phenomena: life-cycle and environmental effects (seasonal change)

Pattern recognition relies on the accurate modeling of statistical properties of population densities. The dynamic nature of living organisms such as cyanobacteria and algae results in properties such as cell area or colony volume being statistically non-stationary (having statistical properties that vary over time, etc.). For example, the average cyanobacterium volume may be quite low during the early stages of a bloom but may be orders of magnitude larger when the bloom has matured. Exceptionally favorable growing conditions may result in uncharacteristically large specimens, resulting in data "outliers." Ultimately, the classification accuracy of an image processing system under these circumstances will rely on the training database capturing as much of this variability as possible. That is, cyanobacteria samples contained in the database should reflect the variability that is found in the natural population. Figure 1 shows two images of *Uroglena americana* colonies at differing stages in their life cycle.

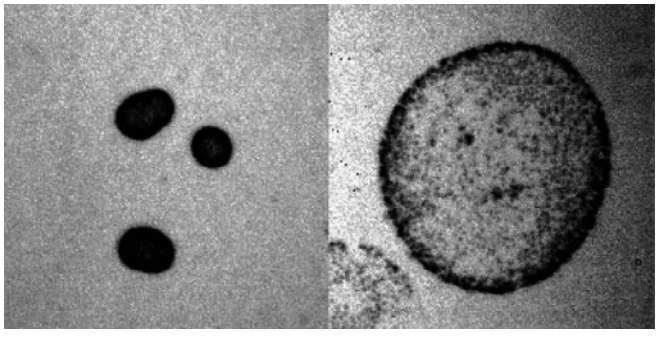

Fig. 1. Intraspecies variation due to natural life cycle. Specimens of *U. americana*, differing in age by 2 weeks, and displayed at the same spatial resolution (2.0 μm), ×10

Intraspecies variation due to predation, fragmentation, etc.

In simple words – body parts. Although algae generally have regular shapes (spherical, spiral, straight, oval), atypical characteristics can occur due to predation, environmental factors, or aging. For example, Fig. 2 shows the deterioration of a *Uroglena americana* colony due to unfavorable environmental conditions.

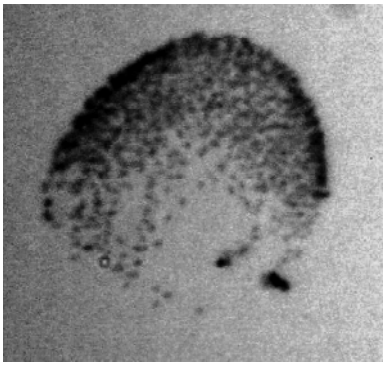

Fig. 2. Intraspecies variation due to damage. This image shows an *U. americana* specimen whose cell colony has started to disintegrate. Characteristics for this colony (such as colony shape and area) will be quite different from the norm, making such characteristics possible statistical outliers. Spatial resolution 2.0 μm, ×10

To stain, or not to stain?

Some species appear clear or opaque at the resolutions used, making imaging and analysis very difficult. Although it is common to stain specimen samples prior to analysis, the staining process itself will negate the goal of fully automated, in-situ, real-time analysis of water samples. A review of the literature suggests that the automated analysis of unstained algae samples is currently rare.

Choosing an appropriate optical resolution for imaging specimens

The wide variation in bulk size of targeted species necessitates a choice of optical magnification that may not be optimal for *any* of the species. For example, to analyze the fine internal structures of species such as *Anabaena*, a spatial resolution of around 0.3 μm is required (Fig. 3). (Spatial resolution is related to the optical microscope's magnification via the imaging camera's pixel *pitch* or spacing, and objective lens magnification.) However, at such a high spatial resolution, *Microcystis* colony specimens generally cannot fit within the microscope's field of view. We have found that a resolution of 2.0 μm provides an unavoidable compromise between imaging large targeted species and fine internal structures. Although a multi-resolution approach is theoretically possible (using two or more objective lenses), the difficulties in manufacturing and implementing such a system are significant. In the future, mega-pixel digital cameras will help to alleviate this problem by removing the requirement for several objective lenses. However, in the meantime, one should ensure that targeted species have bulk properties within an order of magnitude of each other, where possible.

Imaging of three-dimensional objects

Many species have significant length in the third dimension (along the optic or z axis), making their representation as a two-dimensional image difficult. Although *A. smithii* can be easily imaged, species like *A. crassa* (spiral) and *Microcystis* spp**.** (spherical colonies) often have z-axis properties greater than the depth of field of the imaging device (Fig. 4). Therefore, significant areas of the specimen will be out of focus. The equation for an optical microscope's depth-of-field d_f (the in-focus depth along the optic axis, in micrometres) is:

$$d_f = \frac{\lambda}{2(N_a)^2}, \tag{1}$$

where λ is the wavelength of incident light in micrometers and N_a is the numerical aperture of the objective lens. General microscope objective lenses having numerical apertures in the range of 0.3 to 1.3 only provide a focal depth of approximately 0.2 to 3 μm, which is usually too small for imaging thick specimens.

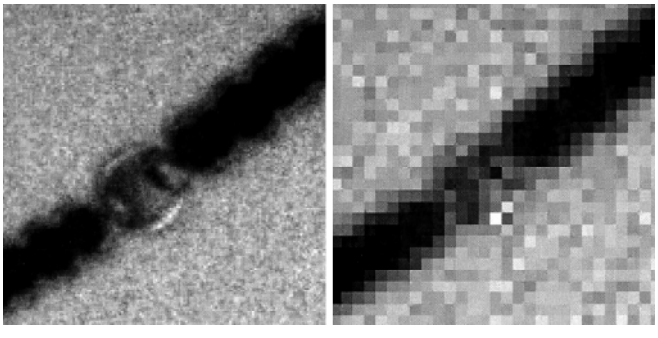

Fig. 3. A portion of *A. smithii*, imaged at a resolution of 0.4 μm (**left**) and 2.0 μm (**right**). Note the loss of fine detail at the lower resolution of 2.0 μm, making measurements such as akinete and heterocyst size or texture analysis difficult. The higher resolution of 0.4 μm tends to be inappropriate for larger species such as *Microcystis*

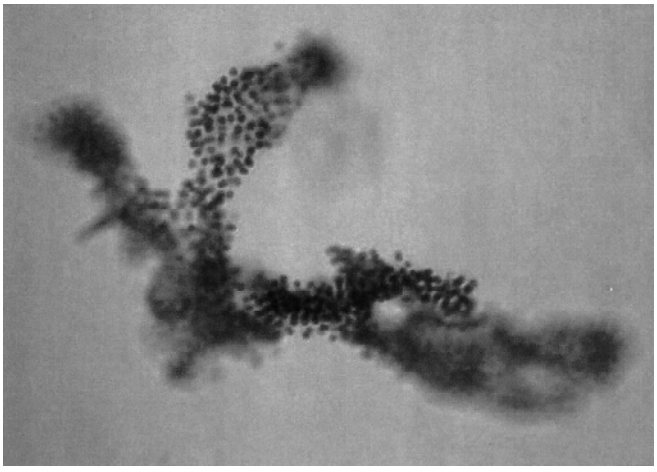

Fig. 4. This image illustrates the difficulties in imaging three-dimensional objects. Notice that several parts of the object (*M. aeruginosa*) are out of focus. Defocused areas may influence the accuracy of statistical measures of image properties. Spatial resolution 0.5 μm, ×40

Water samples will contain a wide range of objects (organic and inorganic), which the system will need to be able to handle. Nontargeted species or objects will generally need to be classified, because it is not known a priori by the system that an object is a nontargeted one. The infinite variability in nontargeted object characteristics means that it is extremely difficult to accurately quantify such characteristics in a statistical sense. This will be perhaps the most difficult problem faced by designers of the image processing system.

Methods

System hardware

The work we present here represents the results of approximately 15 months of system research and development.

Apart from the light microscope, the image processing system has been designed using readily available components, with the aim of keeping the overall system cost to a minimum. A fully self-contained submersible microscope will replace the bench-mounted microscope in the near future, thus allowing fully automated in situ processing of water samples. After training and calibration, the system can now operate almost autonomously. Water sample flow through a water channel cell is currently done manually; however, this operation can be easily automated. Figure 5 shows the system, consisting of purpose-built optical microscope with water sample feed system, high-resolution gray-scale digital imaging camera, digital frame grabber, and image processing computer. Image magnification and focus are controlled via a single remote x-y joystick. However, once appropriate magnification is chosen, it is not varied. Indeed, magnification should not be varied once set, because the reliability of classification depends on all objects being imaged at the same magnification. Sample water is passed as a continuous stream through a channel cell under the microscope's objective. The water channel cell was manufactured with a channel depth of 0.8 mm, to allow for large objects to flow through the cell channel without clogging. However, at the magnification used, the focal depth of the microscope optics was low (≈25 μm). Because we have no control over where in the 0.8-mm channel depth objects will appear, poorly focused objects can and do occur. We handle this problem by measuring the focal accuracy of each image object before processing, and only classifying those objects with adequate focus. We chose to image the lower portion of the 0.8-mm channel depth, because gravity helps to shift floating objects to this level. Digital images of this water are sequentially captured and processed by a high-speed image processing computer. Objects contained within any image are analyzed, and the results of the analysis are stored and displayed. Figure 6 details the general processing steps involved in an image-processing system.

For the purposes of this study, we initially classified image objects as being either from the class "*Microcystis*" or from the class "*Other.*" By the class "*Other*" we mean all image objects that are not from the genus *Microcystis*. Such objects include other cyanobacteria species (*Anabaena flos-aquae*, *A. smithii*, *A. planctonica*, and *A. ucrainica)*, zooplankton, weed, sediment, air bubbles, etc. Because it was not necessary to classify specimens to the species level, an image spatial resolution of 3.5 μm was adequate.

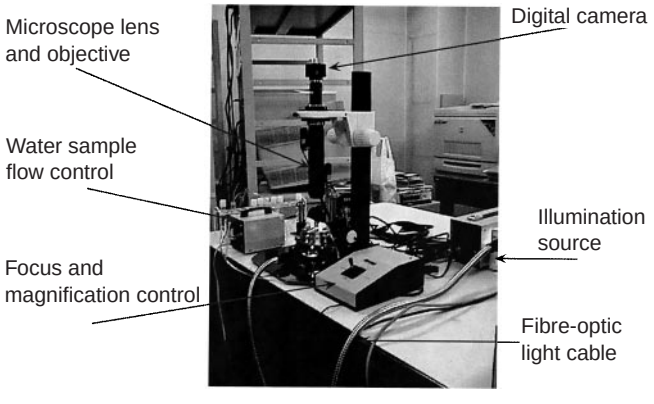

Fig. 5. Microscope and high-resolution digital imaging system. Microscope objective is an Optem Zoom 100 lens with 2× TV tube (N.A. 0.1). The digital camera is a Hitachi KPF100 10-bit gray-scale high-resolution digital camera with pixel density of 1300 × 1024. Images are captured by an Epix PIXCID PCI bus imaging board

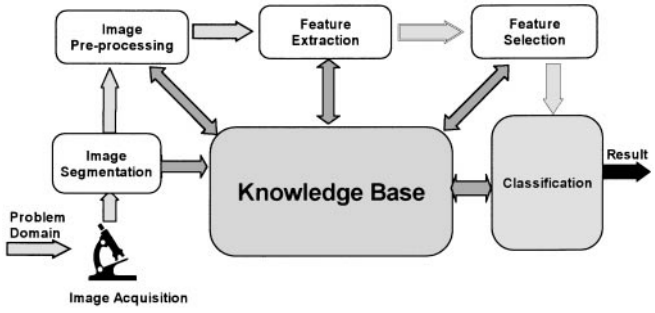

Fig. 6. Processing steps and data flow in a general-purpose image-processing system

To determine the feasibility of a much finer classification, we implemented a second classification process involving a total of seven object classes: *A. flos-aquae*, *A. smithii*, *A. crassa, A. crassa* MIK1, *M. aeruginosa*, *M. wesenbergii*, and "*Other*." (*A. crassa* MIK1 was identified as *A. crassa*, but this strain was isolated from Lake Mikata in Fukui Prefecture, Japan. All other strains were isolated from Lake Biwa.) For this trial, we used images captured at a higher spatial resolution of 0.35 μm. This allowed better characterization of texture properties (higher-order spatial dependencies), which are ideal for discriminating between fine differences in *Microcystis* spp. colony arrangements and *Anabaena* cell-structure properties.

Image-processing methods

Nonuniform illumination correction

Digital images received for analysis are preprocessed to reduce the effects of nonuniform illumination. Such an undesirable characteristic, which represents a nonlinear transformation of the true image intensity data, can present a severe challenge to subsequent image processing algorithms, such as segmentation. In the present system, nonuniform illumination is corrected by using a sequence of blank background images – images that contain no specimens or detritus, etc. These images are pixel-wise averaged to reduce the effects of pixel noise (due both to illumination noise and camera CCD electrical noise). This averaged background image $\bar{I}_B$ is used to filter water sample images I using the following equation:

$$I'(r, c) = I(r, c)\left\{1 + \frac{\bar{I}_{B_{\max}} - \bar{I}_B(r, c)}{\bar{I}_B(r, c)}\right\}, \qquad \forall_{r,c} \qquad (2)$$

where (r, c) represents a valid image pixel co-ordinate pair, $\bar{I}_{B\,\max}$ is the maximum pixel intensity in the averaged back-

ground image, and I' is the resulting filtered image. As a further step to make the system invariant to average illumination intensity variation (which can vary daily or even from image to image, if not specifically set), we apply a further operation,

$$I''(r, c) = \frac{I'(r, c) * 240}{I'_{\max}}, \qquad \forall_{r,c} \tag{3}$$

where I'' is the corrected image, and $I'_{\max}$ is the maximum pixel intensity in I'. This final process normalizes the background intensity of input images to a gray level of 240 (out of a maximum of 256 due to eight-bit photometric resolution), regardless of the microscope's illumination settings. The figure of 240 was chosen to allow a slight buffer between the background intensity of images and image saturation. Figure 7 shows the illumination response of the microscope currently in use.

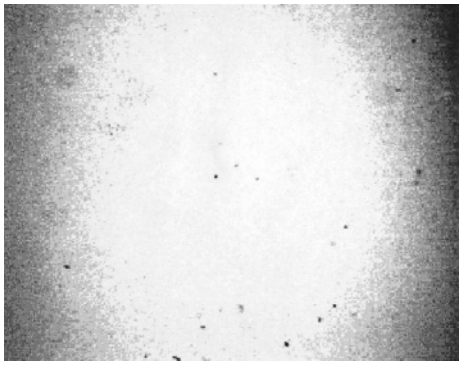

Fig. 7. Illumination response of the microscope (exaggerated). Notice the nonuniform characteristic that can lead to classification inaccuracies if not corrected

Object segmentation

Objects within each image are separated from the image background by forming a binary segmentation *mask* and overlaying this mask on the original gray-scale image. Areas of the image that show through the mask (the objects) are then removed from the image and processed. These steps are performed via morphological image-processing algorithms based on mathematical morphology (Serra 1982; Vincent and Beucher 1989). Because a single image may contain several objects, including multiple species, a fast recursive region extraction algorithm (Chen et al. 1995) was used to sequentially remove each object for subsequent classification. Figure 8 details the segmentation of a typical water sample image.

Focus check

Segmented objects are individually checked to ensure they possess an adequate level of focus. This step is vitally important. As mentioned previously, because the water source

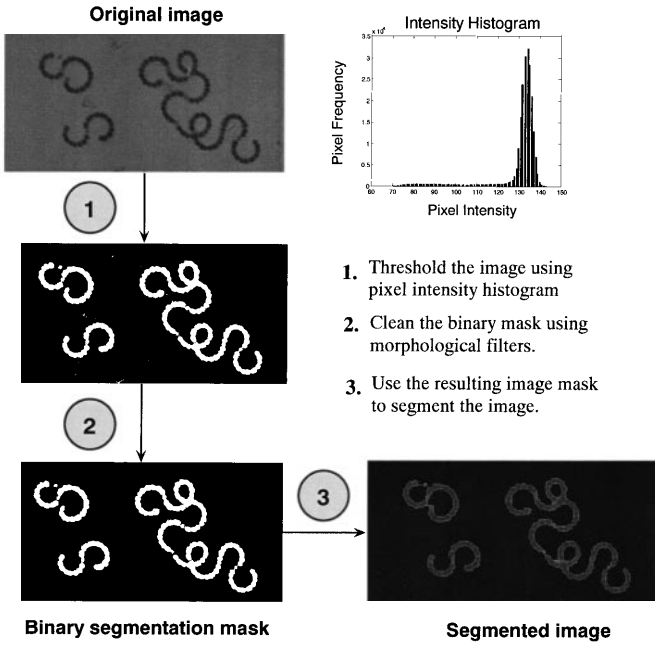

Fig. 8. Segmentation of a typical water sample image

is a three-dimensional column, there is no control over whether an object will fall within the in-focus portion of the microscope's view. As a consequence, there can be great variability in the focal accuracy of objects appearing in the microscope's field of view. Objects with adequate focus are subsequently processed and classified. Objects that do not achieve a minimum average focus limit are analyzed to measure simple characteristics, such as area and shape, but are not subsequently classified. This is because the defocus effect adversely influences many of the statistical properties of the image, and thus may have a strong negative influence on classification accuracy.

Focal quality is measured by removing low spatial frequency components of the object image and averaging the remaining power spectrum across one image dimension (Oliva et al. 1998),

$$F(I) = \sum_r \sum_c \left(h(r) \otimes I(r, c)\right)^2 \Big/ \left(\sum_r \sum_c I(r, c) \Big/ A\right)^2, \tag{4}$$

where $F(I)$ is the focal quality measure for gray-scale image I of spatial domain $A = r_{\max} \times c_{\max}$ pixels, $h(r)$ is the spatial domain response of the one-dimensional highpass filter kernel, and $\otimes$ is the convolution operator. This is a widely used technique and is computationally light, allowing high-speed focal quality measurement.

Object feature extraction

To accurately classify an object into one of several classes (*Microcystis*, *Anabaena*, etc.), it is necessary to quantitatively measure characteristics of the object that may indicate its class membership. For example, the characteristic

"area" is a good discriminator of class membership for classifying *Microcystis* and *Anabaena* cyanobacteria, because these two genera differ substantially in size – *Microcystis* usually being an order of magnitude larger in area. In pattern recognition terms, we call these characteristics "*features*," and the process of measuring an object's characteristics "*feature extraction*."

We measured a total of 123 object features, including morphometric properties, object boundary shape properties, frequency domain properties, and second-order statistical properties. A full list of features can be found in Appendix 1.

Feature selection

Without a priori knowledge, it is difficult to know which of the 123 feature properties will be useful for distinguishing between cyanobacteria species. By the term "useful," we mean features whose statistical properties (mean and variance/covariance, etc.) differ between the various classes of data we are trying to classify. We call such features "discriminatory," in that they can be used to discriminate between classes of data (Fig. 9).

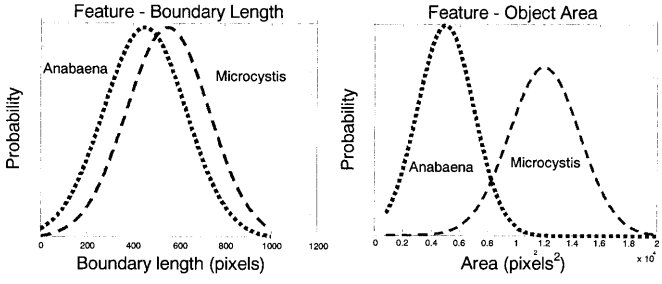

Fig. 9. An example that illustrates discriminatory power. The feature on the **left** possesses low discriminatory power because the two class-conditioned distributions have similar statistics (mean and variance). The one on the **right** possesses high discriminatory power – the two distributions have little overlap. Features whose class-conditioned distributions overlap the least will have greater discriminatory power

To find discriminatory features, we used a feature selection process called sequential forward-selection/backward-elimination (Hand 1981). Specifically, our algorithm iteratively selects two new features and then removes one feature, thus capturing feature pairs that possess higher-order discriminatory power. Kittler (1978) reported that this method almost always gave optimal results and computationally was comparable to less optimal approaches. Using this method, we found that a total of five features from the original set of 123 provided sufficient discriminatory power to classify lower-resolution object data as being either from the classes *Microcystis* or from *Other* (trial 1). For trial 2, where a much finer classification was undertaken (seven classes), discriminant analysis revealed that four features per discriminant function provided sufficient classification performance.

Classification

We performed classification by using a general Bayes decision function for assumed Gaussian feature distributions with unequal variance-covariance matrices (Gonzalez and Woods 1993). The resulting decision surface (where $d_1 = d_2$) is of hyperquadric form:

$$d_i(\mathbf{x}) = \log P_{\omega_i} - \frac{1}{2}\log|\mathbf{C}_i| - \frac{1}{2}\left[(\mathbf{x} - \bar{\mathbf{x}}_i)' \mathbf{C}_i^{-1}(\mathbf{x} - \bar{\mathbf{x}}_i)\right], \quad i = \{1, 2\}, \tag{5}$$

where $\mathbf{x}$ is the feature vector of the object to be classified, $d_i(\mathbf{x})$ represents the discriminant measure for $\mathbf{x}$, P_{ω_i} is the a priori probability of class ω_i, and $\mathbf{C}_i$ and $\bar{\mathbf{x}}_i$ are the variance-covariance matrix and mean vector, respectively, for class i data (determined from a database of objects from known class). For the two-class trial (*Microcystis* vs. *Other*), only one such discriminant function need be determined. For the seven-class trial, classification was implemented by a hierarchy of separate two-class Bayes quadratic classifier units, rather than a single seven-class classifier (Fig. 10). The high similarity of some interclass characteristics means that individual features may not discriminate well among all seven classes. Using a hierarchy of several classifier units allowed the use of several feature sets highly optimized for detecting individual or groups of species. Each classifier was designed by using an optimized subset of four features from the original 123, using sequential-forward-selection/backward-elimination (Kittler 1978).

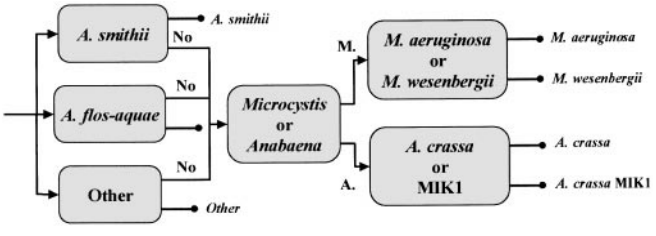

Fig. 10. Multiclass hierarchical classifier structure for trial 2. Using several two-class classifier units (as opposed to a single seven-class classifier) allows each unit to be optimized for the targeted genus/species

Estimating system performance

Measuring classifier performance generally entails quantifying how well the system classifies objects, and is usually expressed in terms of *misclassification rate* or *error rate*, i.e., the rate at which an object is allocated to the wrong object class. In our work, we have used the leave-one-out method to estimate the real error rate. These methods are reviewed in depth in other published literature (Fukunaga 1990; Weiss and Kulikowski 1991), so we will limit our explanation to the basic principles of leave-one-out. Given a dataset of N_s samples, we train the classifier using $N_s - 1$ samples, and test the system using the remaining sample. We repeat this process a total of N_s times, each time leaving out a

different sample, until all samples have been classified once. It is important to note that for leave-one-out, the sample to be classified is not used to train the system, and thus we can obtain an estimate of the real (as opposed to the *apparent*) classification performance of the system.

Results and discussion

Classification results – trial 1

A total of 1529 image objects were extracted from among 1468 images of the five cyanobacteria species. Of these, 1348 were found to have adequate focus and were subsequently classified into the two classes of *Microcystis* or *Other.*

Table 1. Confusion matrix of classification results for trial 1

Species	Classified as Species	
	Microcystis	Other
Microcystis	247	19
Other	12	1070

Table 1 is a confusion matrix of general classification results. The total real error was measured to be 2.3% by using the leave-one-out technique.

In Table 2 we present the classification results in more detail by separating the class "*Other*" into its four constituent species. We notice that the species *A. flos-aquae* has a higher rate of misclassification than the remaining classes. We suspect this is because *A. flos-aquae*, although of spiral shape like *A. ucrainica*, formed itself into very tight, condensed spirals (Fig. 11). As a result, the physical shapes of some *A. flos-aquae* specimens had attributes similar to the dense colonies of *Microcystis* and were subsequently misclassified. However, the nine misclassified samples represent an error rate of only 2.7%, which we feel is sufficiently low. The false-positive rate (misclassifying non-*Microcystis* objects as being *Microcystis*) of only 1.1% is encouragingly low and is advantageous to any system designed specifically to target *Microcystis*.

Table 2. Confusion matrix of classification results, showing species-specific results

Species	Classified as Species	
	Microcystis	Other
M. wesenbergii	247	19
A. flos-aquae	9	322
A. planctonica	0	102
A. smithii	2	336
A. ucrainica	1	310

Classification results – trial 2

We extracted a total of 244 image objects of high focal quality from among 193 images of the six cyanobacteria taxa/strains. Extensive discriminant analysis indicated that three classes – *A. smithii*, *A. flos-aquae*, and *Other* – could be discriminated directly on an individual class basis with sufficient accuracy. (The features for each of these three classes exhibit statistical properties which are sufficiently different from the remaining six classes, thus allowing direct classification.) The four remaining classes were subsequently classified based on genus (*Anabaena* vs. *Microcystis*) and finally on species (*A. crassa* vs. *A. crassa* MIK1; *M. aeruginosa* vs. *M. wesenbergii*) membership. The hierarchical structure of the resulting classifier is detailed in Fig. 10.

Following classifier training, leave-one-out classification was used to provide a robust estimation of the real classification error. A total of seven images were misclassified, indicating an error rate of approximately 3%. These results, in the form of a confusion matrix, are detailed in Fig. 12. Our image processing software GUI is shown in Fig. 13.

An analysis of the database features used to classify each species is warranted. For the two-class classification of "*Microcystis*" vs. "*Other*," the five optimal features used for classification were all GLCM texture measures. The lack of morphological features (such as area) among these five may at first seem surprising – after all, the characteristic shape of *Microcystis* spp. is quite different from that of *Anabaena* spp. However, our feature selection algorithm searches for feature sets that possess higher-order discriminatory power. That is, it searches for features that, as a *team*, discriminate the most. So, although some morphometric features may, individually, discriminate well between the two classes of data, the texture features, in combination, provided an even higher discriminatory power. Also, *Microcystis* spp. cell colony arrangement produces a strong textured appearance that is significantly different from that of the other species, allowing texture features to provide good discrimination.

For the seven-class classification trial, four optimal features were extracted for each of the six classifier units. Of these 24 features, 30% were morphometric features, 5% were boundary shape features, 20% were Fourier boundary features, and 45% were GLCM texture features. Texture features were predominantly used to distinguish *Anabaena* from *Microcystis*, and (as expected) to distinguish between the two *Microcystis* species. It is important to note that, even to a trained bacterial expert, the visual appearances of the two *Microcystis* species are almost identical at the resolution used.

Conclusions

The initial intent of this research was to determine whether it was feasible to automatically classify cyanobacteria species contained in lake or seawater samples by using image-processing and pattern-recognition techniques. If proven

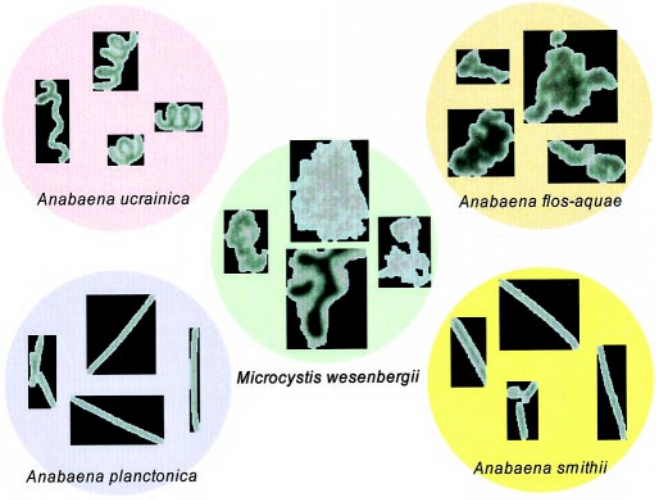

Fig. 11. Examples of individual cyanobacteria that were extracted from high-resolution images, captured using the hardware described in this document

	Classified as class:						
True class	1	2	3	4	5	6	7
1: *A. smithii*	52	0	0	0	0	0	0
2: *A. crassa*	0	41	0	0	0	1	0
3: *A. crassa* MIK1	0	0	45	0	0	0	0
4: *A. flos-aquae*	0	0	0	5	0	0	0
5: *M. aeruginosa*	0	0	0	0	41	0	0
6: *M. wesenbergii*	0	0	0	0	0	41	4
7: Other	0	0	1	0	0	1	12

Fig. 12. Classification results for trial 2 in the form of a confusion matrix. *Rows* indicate the true class, while *columns* indicate classified class

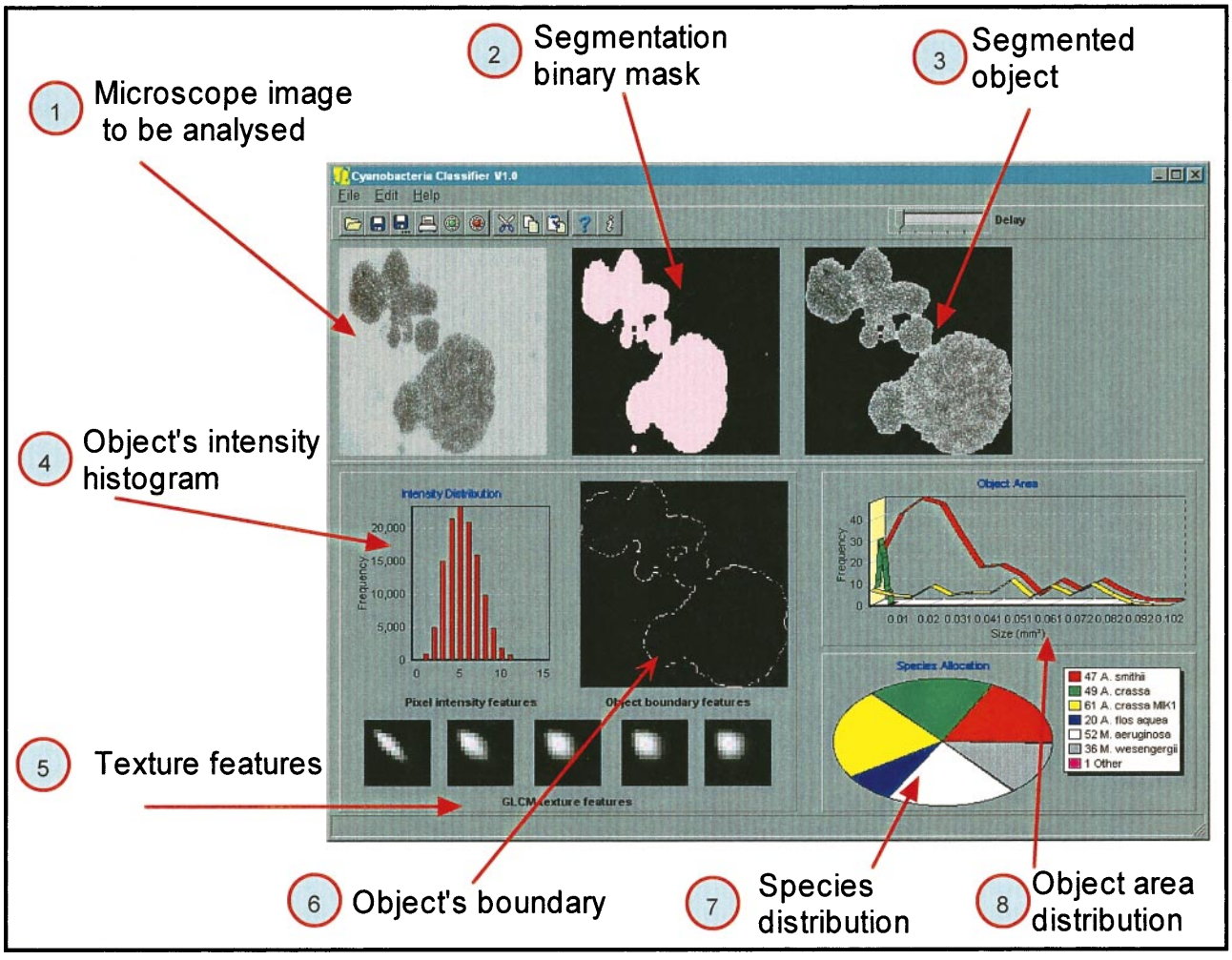

Fig. 13. The image analysis process. (*1*) Microscope image of water sample is transferred to computer for analysis; (*2*) segmentation mask is determined; (*3*) object to be classified is removed from the surrounding image background; (*4–6*) object characteristics are quantitatively measured; (*7*) relative distribution of species numbers found in the water sample; (*8*) distribution of species areas

successful, such a system could be used to augment work currently done by trained bacteria experts, with significant benefits:

Automatic classification can reduce the tedium and fatigue associated with manual classification;
The amount of time required to analyze a sample of water can be significantly reduced;
The expense involved in the purchase of an image-processing system is offset by the significant reduction in labor costs associated with manual classification. In fact, we feel that using such a system will result in considerable cost reductions within several years (or equivalently, higher productivity);
The flexibility of such a system allows for targeted species to be changed at will. The rapid decrease in cost/power ratio for computers will facilitate both an increase in the number of targeted taxonomic groups and more accurate classification via new processing techniques;
Because species are classified using quantitative measures of object characteristics (as opposed to the subjective, qualitative nature of manual classification by trained experts), the system facilitates research by allowing the easy compilation of cyanobacteria characteristics into a database for future reference.

Our work has shown that the extension to classifying multiple species is both straightforward and relatively accurate when abundant images of high quality are used.

The cyanobacteria specimens used in this research were laboratory cultured and may not contain the variability found in lake specimens. Thus the results presented here may degrade somewhat when natural lake water specimens are analyzed. However, we feel that the significantly low error rates reported indicate that automatic classification of cyanobacteria is indeed a feasible and relatively accurate alternative to manual classification.

Acknowledgments The authors wish to thank the Japan Science and Technology Corporation (JST) and the Science and Technology Agency (STA) for providing financial assistance for this project, and the Lake Biwa Research Institute (LBRI) for providing the necessary infrastructure support. We would also like to thank Dr. Tsujimura of LBRI and Yoshiaki Fukunaga of Kistem Ltd. for their technical assistance throughout this work. This paper is dedicated to the memory of Prof. Ryohei Tsuda, whose untimely death in 1996 robbed the research community of a valued colleague.

Appendix 1

List of features extracted from image objects
Morphometric features:
Object area
Object boundary length
Circularity$_1$
Circularity$_2$

Boundary curvature features:
Mean curvature
Minimum curvature
Maximum curvature
Standard deviation of curvature
Number of boundary points with positive curvature

Frequency domain features:
Components 2 to 15 of the one-dimensional complex discrete Fourier transform of object boundary

Texture features:
20 gray level co-occurrence features calculated at five displacements. For a complete description of the texture features, see Walker (1997).

References

Blackburn N, Hagström A, Wikner J, Cuadros-Hansson R, Bjørnsen PK (1998) Rapid determination of bacterial abundance, biovolume, morphology, and growth by neural network-based image analysis. Appl Env Microbiol 64:3246–3255
Chen YQ, Nixon MS, Thomas DW (1995) Statistical geometric features for texture classification. Patt Rec 28:537–552
Estep KW, Macintyre F, Hjörleifsson E, Sieburth J (1986) MacImage: a user-friendly image-analysis system for the accurate mensuration of marine organisms. Mar Ecol 33:243–253
Fukunaga K (1990) Statistical pattern recognition. Academic, New York
Gonzalez RC, Woods RE (1993) Digital image processing. Addison-Wesley, New York
Hand DJ (1981) Discrimination and classification. Wiley, Chichester
Jeffries HP, Berman MS, Poularikas AD, Katsinis C, Melas I, Sherman K, Bivins L (1984) Automated sizing, counting, and identification of zooplankton by pattern Recognition. Mar Biol 78:329–334
Katsinis C, Poularikas AD, Jeffries HP (1984) Image processing and pattern recognition with applications to marine biological images. SPIE 28th Annual International Technical Symposium on Optics and Electro-optics, San Diego, Aug pp 150–155
Kittler J (1978) Feature set search algorithms. In: Chen CH (ed) Pattern recognition and signal processing. Sijthoff and Noordhoff, Alphen ann den Rijn
Kumagai M (1996) Study on climate-induced water quality change in the south basin of Lake Biwa. Lake Biwa Research Institute Bulletin 13:16–19
Nakanishi M (1984) Phytoplankton. In: Horie S (ed) Lake Biwa. Dr W. Junk Publishers, The Hague
Oliva MA, Bravo-Zanoguera M, Price JH (1998) Autofocus for phase-contrast microscopy: investigation of causes of non-unimodality. SPIE Proc Adv Techn Analyt Cytol 3260
Schultze-Lam S, Harauz G, Beveridge T (1992) Participation of a cyanobacterial S layer in fine-grain mineral formation. J Bacteriol 174:7971–7981
Serra J (1982) Image analysis and mathematical morphology. Academic, London
Thiel SU (1994) The use of image processing techniques for the automated detection of blue-green algae. Ph.D. dissertation, University of Glamorgan, UK
Vincent L, Beucher S (1989) The morphological approach to segmentation: an introduction. Mathematische Morphologie und Digitale Bildverarbeitung (Munich):25–27
Walker RF (1997) Adaptive multi-scale texture analysis with application to automated cytology. Ph.D. dissertation, University of Queensland, Australia
Weiss SM, Kulikowski CA (1991) Computer systems that learn: classification and prediction methods from statistics, neural networks, machine learning, and expert systems. Morgan Kaufmann, San Mateo
Wilkins MF, Boddy L, Morris CW, Jonker RR (1999) Identification of phytoplankton from flow cytometry data by using radial basis function neural networks. Appl Env Microbiol 65:4404–4410